Anomalous magnetohydrodynamics with temperature-dependent electric conductivity and application to the global polarization

Hao-Hao Peng, Sihao Wu, Ren-jie Wang,* Duan She,† and Shi Pu‡

Department of Modern Physics, University of Science and Technology of China, Hefei 230026, China

(Received 28 November 2022; accepted 26 April 2023; published 15 May 2023)

We have derived the solutions of the relativistic anomalous magnetohydrodynamics with longitudinal Bjorken boost invariance and transverse electromagnetic fields in the presence of temperature or energy density dependent electric conductivity. We consider the equations of states in a high temperature limit or in a high chiral chemical potential limit. We obtain both perturbative analytic solutions up to the order of $\hbar$ and numerical solutions in our configurations of initial electromagnetic fields and Bjorken flow velocity. Our results show that the temperature or energy density dependent electric conductivity play an important role to the decaying of the energy density and electromagnetic fields. We also implement our results to the splitting of global polarization for Λ and $\bar{\Lambda}$ hyperons induced by the magnetic fields. Our results for the splitting of global polarization disagree with the experimental data in low energy collisions, which implies that the contribution from electromagnetic fields may be insufficient to explain the global polarization of Λ and $\bar{\Lambda}$ hyperons in the low energy collisions.

DOI: 10.1103/PhysRevD.107.096010

I. INTRODUCTION

Recently, strong electromagnetic (EM) fields (of order 10^{17}–10^{18} Gauss [1–4]) generated in the relativistic heavy ion collisions provide a platform to study the novel quantum transport phenomena and nonlinear quantum electrodynamics.

The strong magnetic fields can induce the chiral magnetic effect (CME) [5–8] associated with the chiral anomaly, chiral separation effect [9] and chiral magnetic wave [10,11]. While the electric fields can cause chiral electric separation effect [12–15] and other novel nonlinear EM responses in chiral systems [15–20]. These chiral transport phenomena are naturally connected to the Schwinger mechanism [21–25]. More discussions and references can be found in recent reviews [26–35]. To understand and describe these chiral transport, the quantum kinetic theory or named Wigner function approaches, as an microscopic effective theory has been widely discussed [36–73] (also see Refs. [34,72,74] for the recent reviews on quantum kinetic theory).

It is still challenging to search the CME signal in the relativistic heavy ion collision at Relativistic Heavy Ion Collider (RHIC) [75–82] and Large Hadron Collider (LHC) [83–85]. Although many possible correlators or observables have been proposed [78], the background contributions from, e.g., the transverse momentum conservation [86–90], local charge conservation [91] and nonflow correlations [92,93], cannot be neglected. Nevertheless, the recent isobar collisions [94] in STAR measurements [95] do not observe the CME signature that satisfies the predefined criteria. It requires the future systematical studies on CME.

Another interesting phenomena related to the chiral transport and EM fields is the global and local polarization of Λ and $\bar{\Lambda}$ hyperons [96–98]. The global polarization has been measured by the STAR experiments [99] and been widely studied in several models [100–110] (also see recent reviews [34,111–113]). Meanwhile, the local spin polarization, in $\mathrm{Au}+\mathrm{Au}$ collisions at $\sqrt{s_{NN}}=200$ GeV has been measured [114] and studied [109,110,115–119]. Several studies have pointed out that the splitting of global polarization of Λ and $\bar{\Lambda}$ hyperons may be induced by the EM fields [120–123] and gradient of baryon chemical potential [109,110,124]. Therefore, the further studies on the EM fields and their evolution are also required in this field.

On the other hand, strong EM fields make the studying of the nonlinear electrodynamics be possible. The light-by-light scattering [125], matter generation directly from photons [126,127], the vacuum birefringence [126,128–132] have

*wrjn@mail.ustc.edu.cn
†sheduan@ustc.edu.cn
‡shipu@ustc.edu.cn

been measured. People find that the EM fields can be considered as the real photons approximations. Therefore, the lepton pair photoproduction in peripheral and ultra-peripheral collisions have been comprehensively studied at both experimental [126,133–135] and theoretical sides, e.g., by the generalized equivalent photon approximation or the calculations based on QED models in the background field approaches [127,136–142], the framework based on the factorization theorem [143–146] and the calculation based on QED with the assumption of wave packet [147–149].

As known, the relativistic hydrodynamics [150–157] is an macroscopic effective theory for the relativistic many body systems. To learn the chiral transport phenomena, the relativistic anomalous magentohydrodynamics (MHD), which are the ordinary relativistic hydrodynamics coupled to the Maxwell's equation in the presence of chiral anomaly and CME, has been widely discussed [158–167]. Meanwhile, the simulations from the anomalous-viscous fluid dynamics with a given background EM fields are presented in Refs. [168–170]. Similarly, to describe the polarization effects, the spin hydrodynamics have been built [171–197] (also see the recent reviews [34,111–113,176,198]).

In previous studies [162,163] by some of us, we have investigated the relativistic anomalous MHD with a longitudinal boost invariant Bjorken flow and transverse EM fields. For simplicity, we assume the electric conductivity is a constant. Nevertheless, the recent numerical simulations from relativistic Boltzmann equations show that the electric conductivity changes with proper time [199–202]. To consider these effects, we need to consider a temperature dependent electric conductivity, also see the early studies from lattice QCD [203–205] and holographic models [13,15]. We will solve the anomalous MHD in a longitudinal boost invariant Bjorken flow with a temperature or energy density dependent electric conductivity. Meanwhile, we will implement our results to the splitting of global polarization for the Λ and $\bar{\Lambda}$ hyperons.

The structure of this work is as follows. In Sec. II, we briefly review the relativistic anomalous MHD. Then, we consider two kinds of equations of state, which are the system in a high temperature or high chiral chemical potential limits and take the system in a Bjorken flow in Sec. III. We present the perturbative analytic solutions and numerical solutions with our configurations of initial EM fields in high temperature and high chiral chemical potential limits in Sec. IV and V, respectively. We implement our results to the splitting of global polarization of Λ and $\bar{\Lambda}$ hyperons in Sec. VI and summarize the work in Sec. VII.

Throughout this work, we choose the metric $g_{\mu\nu} = \mathrm{diag}\{+,-,-,-\}$ and Levi-Civita tensor $\epsilon^{\mu\nu\rho\sigma}$ satisfying $\epsilon^{0123} = -\epsilon_{0123} = +1$. Note that $\epsilon^{\mu\nu\alpha\beta}\epsilon_{\mu\nu\rho\sigma} = -2!(g^{\alpha}_{\rho}g^{\beta}_{\sigma} - g^{\alpha}_{\sigma}g^{\beta}_{\rho})$. The fluid velocity $u^{\mu} = \gamma(1,\mathbf{v})$ with γ being Lorentz factor satisfies $u^{\mu}u_{\mu} = 1$ and $\Delta^{\mu\nu} = g^{\mu\nu} - u^{\mu}u^{\nu}$ is the orthogonal projector to the fluid four-velocity u^{μ}.

II. ANOMALOUS MAGNETOHYDRODYNAMICS

In this section, we give a brief review for the relativistic anomalous MHD. The MHD equations are the conservation equations coupled to the Maxwell's equations (see, e.g., Refs. [158–163,206–208]). The energy-momentum conservation equation is,

$$\partial_{\mu}T^{\mu\nu} = 0, \tag{1}$$

where the energy-momentum tensor $T^{\mu\nu}$ can be decomposed as two parts,

$$T^{\mu\nu} = T^{\mu\nu}_{F} + T^{\mu\nu}_{\mathrm{EM}}. \tag{2}$$

Here, $T^{\mu\nu}_{F}$ stands for the energy-momentum tensor of the medium and is usually written as in the Landau frame,

$$T^{\mu\nu}_{F} = \varepsilon u^{\mu}u^{\nu} - (p+\Pi)\Delta^{\mu\nu} + \pi^{\mu\nu}, \tag{3}$$

where $\varepsilon, p, \Pi, \pi^{\mu\nu}$ denote the energy density, pressure, bulk viscosity pressure and shear viscous tensor, respectively. The $T^{\mu\nu}_{\mathrm{EM}}$ is the energy and momentum given by the EM fields, i.e.,

$$T^{\mu\nu}_{\mathrm{EM}} = -F^{\mu\lambda}F^{\nu}_{\lambda} + \frac{1}{4}g^{\mu\nu}F^{\rho\sigma}F_{\rho\sigma}. \tag{4}$$

In the relativistic hydrodynamics, we usually rewrite the EM tensor $F^{\mu\nu}$ as,

$$F^{\mu\nu} = E^{\mu}u^{\nu} - E^{\nu}u^{\mu} + \epsilon^{\mu\nu\alpha\beta}u_{\alpha}B_{\beta}, \tag{5}$$

where we introduce the four vector form of electric and magnetic fields,

$$E^{\mu} = F^{\mu\nu}u_{\nu}, \qquad B^{\mu} = \frac{1}{2}\epsilon^{\mu\nu\alpha\beta}u_{\nu}F_{\alpha\beta}. \tag{6}$$

Note that, by definition (6), we find that $u^{\mu}E_{\mu} = 0$ and $u^{\mu}B_{\mu} = 0$. For convenience, we also define

$$E = \sqrt{-E^{\mu}E_{\mu}}, \qquad B = \sqrt{-B^{\mu}B_{\mu}}. \tag{7}$$

Besides the energy and momentum conservation, we have the charge (or vector current) j^{μ}_{e} conservation equations and the anomalous equations for the axial current (or chiral current) j^{μ}_{5},

$$\partial_{\mu}j^{\mu}_{e} = 0, \qquad \partial_{\mu}j^{\mu}_{5} = -e^{2}CE^{\mu}B_{\mu}. \tag{8}$$

Here, $C = \hbar/(2\pi^{2})$ is the chiral anomaly coefficient [162,163,209–212]. The constitutive equations for the currents are,

$$j_e^\mu = n_e u^\mu + \sigma E^\mu + \xi B^\mu + \xi_\omega \omega^\mu + \nu^\mu,$$
$$j_5^\mu = n_5 u^\mu + \sigma_5 E^\mu + \xi_5 B^\mu + \xi_{5\omega}\omega^\mu + \nu_5^\mu. \quad (9)$$

Here, n_e and n_5 are the electric and chiral charge density, respectively. The ν^μ, ν_5^μ are the heat conducting flow for the charge and chiral currents, respectively. The transport coefficients for conducting flows induced by the electric fields σ, σ_5 are computed by Refs. [12,13,15]. The transport coefficients for the CME and chiral separation effect ξ and ξ_5 are [8,36,38],

$$\xi = eC\mu_5, \qquad \xi_5 = eC\mu_e, \quad (10)$$

where μ_e and μ_5 are the chemical potentials for the charge and chiral charge, respectively. The terms $\xi_\omega\omega^\mu$ and $\xi_{5\omega}\omega^\mu$ denote the chiral vortical effect and the chiral current induced by the vortical fields [8,36,38], with $\omega^\mu = \frac{1}{2}\epsilon^{\mu\nu\alpha\beta}u_\nu\partial_\alpha u_\beta$, being the vortical field.

Two types of Maxwell's equations are

$$\partial_\mu F^{\mu\nu} = j_e^\nu,$$
$$\partial_\mu(\epsilon^{\mu\nu\alpha\beta}F_{\alpha\beta}) = 0. \quad (11)$$

Or, we can rewrite Eqs. (11) in the terms of E^μ and B^μ,

$$\partial_\mu(E^\mu u^\nu - E^\nu u^\mu + \epsilon^{\mu\nu\alpha\beta}u_\alpha B_\beta) = j_e^\nu,$$
$$\partial_\mu(B^\mu u^\nu - B^\nu u^\mu + \epsilon^{\mu\nu\alpha\beta}u_\beta E_\alpha) = 0. \quad (12)$$

The thermodynamic relations and Gibbs relations read,

$$\varepsilon + p = Ts + \mu n + \mu_5 n_5,$$
$$d\varepsilon = Tds + \mu dn + \mu_5 dn_5. \quad (13)$$

Note that, in general, the EM fields can modify the above relations through the magnetization and electric polarization [158]. Here, we neglect these higher order corrections. Besides Eqs. (13), we also need the equations of state (EoS) to close the whole system.

In Ref. [162], the electric conductivity σ is assumed as a constant. However, in general, the electric conductivity depends on both temperature and chemical potential and is changed with the evolution of the system. Therefore, in the current study, we consider a temperature and/or energy density dependent conductivity σ.

III. EQUATIONS IN A BJORKEN FLOW

In this section, we introduce two equations of state (EoS) and consider the initial system is in a Bjorken flow.

We follow Refs. [158–163] to search the solutions in a force-free MHD. We need to simplify the main equations for MHD. First, we neglect the standard dissipative terms in $T^{\mu\nu}$ and currents j^μ, j_5^μ, i.e., we set $\Pi = \pi^{\mu\nu} = \nu^\mu = \nu_5^\mu = 0$. Second, although the vortical fields ω^μ is of importance to the spin polarization in the relativistic heavy ion collisions (see the recent reviews [34,72] and the references therein), it is not directly connected to the evolution of EM fields. Therefore, we also neglect the terms proportional to ω^μ in the currents (9) for simplicity. Third, from the Maxwell's equations, we know the charged fluid cells will be accelerated by the EM fields. To search for the force-free type solutions in Ref. [158–163], we assume that the fluid is charge neutral, i.e., we set $\mu_e = n_e = 0$. Since the chiral electric conductivity σ_5 is proportional to $\mu_e\mu_5$ [12,13,15] in the small chemical potentials limits, we find that $\sigma_5 = 0$ under the assumption of vanishing μ_e.

We consider two typical EoS to close the system.

In the high temperature limit, the EoS labeled as "EOS-HT" is assumed as

$$\varepsilon = c_s^{-2}p,$$
$$n_5 = a\mu_5 T^2, \quad (14)$$

where speed of sound c_s and a are dimensionless constants. For an ideal fluid, $c_s^2 = a = 1/3$ for instance [213]. In the high temperature limit, the electric conductivity is assumed to be proportional to temperature T due to the dimension analysis, i.e.,

$$\sigma = \sigma_0\left[\frac{T(\tau)}{T(\tau_0)}\right] + \mathcal{O}\left(\frac{\mu_5}{T}\right), \quad (15)$$

with σ_0 being a constant, τ is the proper time and τ_0 being the initial proper time.

In the high chiral chemical potential limit, we label the EoS as "EOS-HC", which is given by,

$$\varepsilon = c_s^{-2}p,$$
$$n_5 = a\mu_5^3. \quad (16)$$

In the ideal fluid limit, $a = 1/(3\pi^2)$ [36,213]. The electric conductivity is assumed to be, $\sigma \propto (\mu_e^2 + \mu_5^2)/T$, i.e.,

$$\sigma = \sigma_0\left[\frac{n_5(\tau)}{n_5(\tau_0)}\right]^{2/3}\left[\frac{\varepsilon(\tau_0)}{\varepsilon(\tau)}\right]^{c_s^2/(1+c_s^2)} + \mathcal{O}(T/\mu, T/\mu_5). \quad (17)$$

Note that, for simplicity, we replace the temperature dependence by the energy density dependent in Eq. (17). More systematical discussions on the electric conductivity can be found in lattice QCD [203,204], perturbative QCD at finite temperature and chemical potentials and holographic models [214] and other models [205].

We summarize the main differential equations. The Eqs. (1), (8), (11) with the constitutive equations (3), (9), the EoS (14) or (16) with thermodynamic relations (13) and electric conductivity (15) or (17) are the main equations for the anomalous MHD. The acceleration equations for the fluid velocity, i.e., $\Delta_{\mu\alpha}\partial_\nu T^{\mu\nu} = 0$, gives,

$$(u\cdot\partial)u_\alpha=\frac{1}{\varepsilon+p+E^2+B^2}\left[\Delta_\alpha{}^\nu\partial_\nu\left(p+\frac{1}{2}E^2+\frac{1}{2}B^2\right)+\Delta_{\mu\alpha}(E\cdot\partial)E^\mu+E_\alpha(\partial\cdot E)+\Delta_{\mu\alpha}(B\cdot\partial)B^\mu\right.$$
$$\left.+B_\alpha(\partial\cdot B)+\epsilon^{\nu\lambda\rho\sigma}E_\lambda B_\rho u_\sigma(\partial_\nu u_\alpha)+(\partial\cdot u)\epsilon_{\alpha\lambda\rho\sigma}E^\lambda B^\rho u^\sigma+\Delta_{\mu\nu}(u\cdot\partial)\epsilon^{\mu\lambda\rho\sigma}E_\lambda B_\rho u_\sigma\right]. \tag{18}$$

The total energy conservation equation $u_\mu\partial_\nu T^{\mu\nu}=0$ reads,

$$(u\cdot\partial)\left(\varepsilon+\frac{1}{2}E^2+\frac{1}{2}B^2\right)+(\varepsilon+p+E^2+B^2)(\partial\cdot u)$$
$$=u_\mu(E\cdot\partial)E^\mu+u_\mu(B\cdot\partial)B^\mu+\epsilon^{\nu\lambda\rho\sigma}\partial_\nu(E_\lambda B_\rho u_\sigma)+u_\mu(\partial\cdot u)\epsilon^{\mu\lambda\rho\sigma}E_\lambda B_\rho u_\sigma. \tag{19}$$

The conservation equations (8) becomes,

$$\partial_\mu(\sigma E^\mu+\xi B^\mu)=0,$$
$$\partial_\mu(n_5u^\mu)=0. \tag{20}$$

The charge conservation equation in the first line of Eq. (20) can also be derived from the Maxwell's equation, therefore, it is not an independent dynamical equation for EM fields. The explicit expression for the Maxwell's equations (12) under our assumptions is,

$$\partial_\mu(E^\mu u^\nu-E^\nu u^\mu+\epsilon^{\mu\nu\alpha\beta}u_\alpha B_\beta)=\sigma E^\nu+\xi B^\nu,$$
$$\partial_\mu(B^\mu u^\nu-B^\nu u^\mu+\epsilon^{\mu\nu\alpha\beta}u_\beta E_\alpha)=0. \tag{21}$$

We follow the basic idea in Refs. [158–163] to search for the analytic solutions in our cases. We assume that the fluid is a Bjorken flow initially. We introduce the Milne coordinates

$$z=\tau\sinh\eta,\qquad t=\tau\cosh\eta, \tag{22}$$

where

$$\tau=\sqrt{t^2-z^2},$$
$$\eta=\frac{1}{2}\ln\left(\frac{t+z}{t-z}\right), \tag{23}$$

are the proper time and the space-time rapidity, respectively. The fluid velocity of a longitudinal boost invariant Bjorken flow is given by [215],

$$u^\mu=(\cosh\eta,0,0,\sinh\eta)=\gamma(1,0,0,z/t). \tag{24}$$

For simplicity, we also assume the initial E^μ and B^μ depends on τ only and are parallel or antiparallel to the each other. Without loss of generality, we set the initial EM field be put in the y direction only,

$$E^\mu=(0,0,\chi E(\tau),0),\qquad B^\mu=(0,0,B(\tau),0), \tag{25}$$

where $\chi=\pm1$ represent parallel or antiparallel. Following the standard conclusion in a Bjorken flow, we also assume that all the thermodynamic quantities depend on proper time τ only at the initial time τ_0.

We first assume that during the evolution the EM fields are still satisfying the profile (25) and the thermodynamic variables still depend on the proper time only and then check whether this assumption can always be satisfied. The acceleration equation (18) reduces to $(u\cdot\partial)u_\alpha=0$, i.e., the fluid will not be accelerated by the EM fields. The Maxwell's equations (21) reduce to,

$$(u\cdot\partial)E+E(\partial\cdot u)+\sigma E+\chi\xi B=0,$$
$$(u\cdot\partial)B+B(\partial\cdot u)=0. \tag{26}$$

The equations for energy conservation and chiral anomaly becomes, under these assumptions and with the help of Eq. (26),

$$(u\cdot\partial)\varepsilon+(\varepsilon+p)(\partial\cdot u)-\sigma E^2-\chi\xi EB=0,$$
$$(u\cdot\partial)n_5+n_5(\partial\cdot u)-e^2C\chi EB=0. \tag{27}$$

Although one can automatically derive the charge conservation equation from Maxwell's equation, let us still check whether the charge conservation equation (20) as a constrain equation for EM fields can be satisfied or not. With our configurations for the transverse EM fields in Eq. (25) and the our assumption for conductivities in Eq. (15) or (17), it is straightforward to obtain $\partial_\mu j^\mu=\partial_\mu(\sigma E^\mu+\xi B^\mu)=0$. Combining Eqs. (26) and (27), we can conclude that with the initial configurations (25), the initial fluid velocity (24) holds and all the thermodynamic variables will always depend on the proper time only during the evolution.

Note that we do not take the EM fields as the background fields. In a background EM fields approach, all the possible acceleration given by EM fields or back reactions from fluid cells are neglected. Here, we are searching for the

configurations of EM fields to satisfy the force-free condition, i.e., the EM fields will not accelerate the fluid cells.

Before end of this section, we would like to emphasize the E^μ and B^μ in Eq. (25) are defined in a comoving frame. The electromagnetic fields $\mathbf{E_{lab}}$ and $\mathbf{B_{lab}}$ in the laboratory frame can be obtained through $F^{\mu\nu}$ directly,

$$\begin{aligned}\mathbf{E}_{\rm lab} &= (\gamma v^z B(\tau), \chi\gamma E(\tau), 0),\\ \mathbf{B}_{\rm lab} &= (-\gamma v^z \chi E(\tau), \gamma B(\tau), 0).\end{aligned} \tag{28}$$

In the ideal MHD limit, i.e., $\sigma \to 0$, since $j^\mu \sim \sigma E^\mu$ should be finite, E^μ vanish. Therefore, the magnetic fields in lab frame will reduce to $\mathbf{B}_{\rm lab} = (0, \gamma B(\tau), 0)$.

In next section, we will solve Eqs. (26), (27). Interestingly, there are no terms proportional to $\partial_\mu\sigma$ in Eqs. (26), (27), i.e., Eqs. (26), (27) are the same as those in the case of constant σ. We emphasize that now the σ depends on proper time, e.g., in Eq. (15) for EoS-HT (14) and Eq. (17) for EoS-HC (16). Therefore, the system evolution becomes more complicated then those in Ref. [162,163].

IV. SOLUTIONS IN HIGH TEMPERATURE LIMIT

In this section, we solve the simplified differential equations (26), (27) with the EoS-HT (14) and temperature dependent conductivity (15).

Following Refs. [162,163,165,216], we implement the following method. For a given differential equation

$$\left(\frac{d}{d\tau} + \frac{m}{\tau}\right) f(\tau) = f(\tau)\frac{d}{d\tau}\lambda(\tau), \tag{29}$$

with m being a constant and $\lambda(\tau)$ being a given source term, the solution for $f(\tau)$ can be written in a compact form,

$$f(\tau) = f(\tau_0)\exp[\lambda(\tau) - \lambda(\tau)]\left(\frac{\tau_0}{\tau}\right)^m, \tag{30}$$

where τ_0 is an initial proper time and $f(\tau_0)$ is the initial value of $f(\tau)$ at τ_0.

From Eq. (26) it is straightforward to get

$$B(\tau) = B_0\frac{\tau_0}{\tau}, \tag{31}$$

where B_0 is initial magnetic fields.

We rewrite Eqs. (26), (27) in a compact form,

$$\begin{aligned}\frac{d}{d\tau}\varepsilon + (1+c_s^2)\frac{\varepsilon}{\tau} &= \varepsilon\frac{d}{d\tau}\mathcal{L},\\ \frac{d}{d\tau}E + \frac{E}{\tau} &= E\frac{d}{d\tau}\mathcal{E},\\ \frac{d}{d\tau}n_5 + \frac{n_5}{\tau} &= n_5\frac{d}{d\tau}\mathcal{N},\end{aligned} \tag{32}$$

where the source terms are given by,

$$\begin{aligned}\frac{d}{d\tau}\mathcal{L} &= \frac{1}{\varepsilon}\sigma E^2 + \frac{1}{\varepsilon}eC\chi\mu_5 EB,\\ \frac{d}{d\tau}\mathcal{E} &= -\sigma - eC\chi\mu_5\frac{B}{E},\\ \frac{d}{d\tau}\mathcal{N} &= \frac{e^2C\chi EB}{n_5}.\end{aligned} \tag{33}$$

Following Eq. (30), the solutions of Eqs. (32) read,

$$\begin{aligned}E(\tau) &= E_0\left(\frac{\tau_0}{\tau}\right)\exp[\mathcal{E}(\tau) - \mathcal{E}(\tau_0)] \equiv E_0\left(\frac{\tau_0}{\tau}\right)x(\tau),\\ n_5(\tau) &= n_{5,0}\left(\frac{\tau_0}{\tau}\right)\exp[\mathcal{N}(\tau) - \mathcal{N}(\tau_0)] \equiv n_{5,0}\left(\frac{\tau_0}{\tau}\right)y(\tau),\\ \varepsilon(\tau) &= \varepsilon_0\left(\frac{\tau_0}{\tau}\right)^{1+c_s^2}\exp[\mathcal{L}(\tau) - \mathcal{L}(\tau_0)] \equiv \varepsilon_0\left(\frac{\tau_0}{\tau}\right)^{1+c_s^2}z(\tau),\end{aligned} \tag{34}$$

where $E_0, n_{5,0}, \varepsilon_0$ are initial electric field, chiral density and energy density at $\tau = \tau_0$ and we have introduced three variables $x(\tau)$, $y(\tau)$ and $z(\tau)$,

$$\begin{aligned}x(\tau) &= \exp[\mathcal{E}(\tau) - \mathcal{E}(\tau_0)],\\ y(\tau) &= \exp[\mathcal{N}(\tau) - \mathcal{N}(\tau_0)],\\ z(\tau) &= \exp[\mathcal{L}(\tau) - \mathcal{L}(\tau_0)].\end{aligned} \tag{35}$$

In the high temperature limit, the energy density can be written in the power series of $\mu_5/T \ll 1$,

$$\varepsilon(\tau) = \varepsilon_0\left(\frac{T}{T_0}\right)^{1+c_s^{-2}} + \mathcal{O}\left(\frac{\mu_5^2}{T^2}\right). \tag{36}$$

From Eq. (34) for energy density ε, we get

$$T = T_0\left(\frac{\tau_0}{\tau}\right)^{c_s^2} z(\tau)^{c_s^2/(1+c_s^2)}. \tag{37}$$

and, from Eq. (15),

$$\sigma = \sigma_0 \left(\frac{\tau_0}{\tau}\right)^{c_s^2} z(\tau)^{c_s^2/(1+c_s^2)}. \tag{38}$$

Inserting the expression for x, y, z into Eqs. (33), yields,

$$\begin{aligned}
\frac{d}{d\tau}x &= -\sigma_0 \left(\frac{\tau_0}{\tau}\right)^{c_s^2} x z^{c_s^2/(1+c_s^2)} - \frac{a_1}{\tau_0}\left(\frac{\tau_0}{\tau}\right)^{1-2c_s^2} y z^{-2c_s^2/(1+c_s^2)}, \\
\frac{d}{d\tau}y &= a_2 \frac{x}{\tau}, \\
\frac{d}{d\tau}z &= \frac{E_0^2}{\varepsilon_0}\sigma_0 \left(\frac{\tau_0}{\tau}\right) x^2 z^{c_s^2/(1+c_s^2)} \\
&\quad + \frac{a_1}{\tau_0}\left(\frac{E_0^2}{\varepsilon_0}\right)\left(\frac{\tau_0}{\tau}\right)^{2-3c_s^2} x y z^{-2c_s^2/(1+c_s^2)},
\end{aligned} \tag{39}$$

where by definition, $x(\tau_0) = y(\tau_0) = z(\tau_0) = 1$, and $a_{1,2}$ are all dimensionless constants determined by the initial conditions

$$\begin{aligned}
a_1 &= eC\chi \frac{B_0 n_{5,0}}{a T_0^2 E_0}\tau_0, \\
a_2 &= e^2 C\chi \frac{E_0 B_0}{n_{5,0}}\tau_0.
\end{aligned} \tag{40}$$

We notice that $a_{1,2} \propto C \sim \hbar$ and it denotes that the terms proportional to a_1, a_2 in Eqs. (39) are quantum corrections to the ordinary MHD.

From the numerical simulations in Ref. [4], we find that the initial energy density of fluid ε_0 is much larger than the initial energy density of EM fields $\varepsilon_0 \gg E_0^2, B_0^2, E_0 B_0$. For simplicity, we consider $\mathcal{O}(\frac{E_0^2}{\varepsilon_0}) \sim \mathcal{O}(a_{1,2}) \sim \mathcal{O}(\hbar)$. To the leading order of $\hbar$, we get the solutions for Eqs. (39),

$$\begin{aligned}
x(\tau) &= e^{m_1(\tilde{\tau}-1)} - a_1 e^{m_1\tilde{\tau}}(1-c_s^2)^{-1}[\mathcal{E}(n_1, m_1) - \tilde{\tau}^{-2c_s^2/(c_s^2-1)}\mathcal{E}(n_1, m_1\tilde{\tau})], \\
y(\tau) &= 1 + a_2 e^{-m_1}(1-c_s^2)^{-1}[\mathcal{E}(1, -m_1) - \mathcal{E}(1, -m_1\tilde{\tau})], \\
z(\tau) &= 1 - \frac{E_0^2}{\varepsilon_0} m_1 e^{-2m_1}[\mathcal{E}(1, -2m_1) - \mathcal{E}(1, -2m_1\tilde{\tau})] + a_1 \frac{E_0^2}{\varepsilon_0} e^{-m_1}(1-c_s^2)^{-1}[\mathcal{E}(2n_2, -m_1) - \tilde{\tau}^{(1-3c_s^2)/(c_s^2-1)}\mathcal{E}(2n_2, -m_1\tilde{\tau})],
\end{aligned} \tag{41}$$

where

$$\mathcal{E}(n, m) \equiv \int_1^\infty dt t^{-n} e^{-mt}, \tag{42}$$

is the generated exponential integral, and

$$\begin{aligned}
n_1 &= \frac{1-3c_s^2}{1-c_s^2}, \\
n_2 &= \frac{1-2c_s^2}{1-c_s^2}, \\
m_1 &= -\frac{\sigma_0\tau_0}{1-c_s^2}, \\
\tilde{\tau} &= \left(\frac{\tau_0}{\tau}\right)^{c_s^2-1}.
\end{aligned} \tag{43}$$

Inserting the solutions for x, y, z back into Eqs. (34), we can get the solutions for $E(\tau), n_5(\tau)$ and $\varepsilon(\tau)$.

In the order of $\hbar^0$, we find,

$$\begin{aligned}
E(\tau) &= E_0\left(\frac{\tau_0}{\tau}\right)x(\tau) \propto \frac{1}{\tau}e^{-\sigma(\tau)\tau}, \\
n_5(\tau) &= n_{5,0}\left(\frac{\tau_0}{\tau}\right)y(\tau) \propto \frac{\tau_0}{\tau}, \\
\varepsilon(\tau) &= \varepsilon_0\left(\frac{\tau_0}{\tau}\right)^{1+c_s^2} z(\tau) \propto \left(\frac{\tau_0}{\tau}\right)^{1+c_s^2},
\end{aligned} \tag{44}$$

which are consistent with the results in a ordinary MHD with finite electric conductivity in a Bjorken flow as discussed by Refs. [162,163]. We also find that,

$$\sigma(\tau) = \sigma_0\left[\frac{T(\tau)}{T(\tau_0)}\right] \propto \left(\frac{\tau_0}{\tau}\right)^{c_s^2}, \tag{45}$$

which decays with proper time. The numerical studies of $\sigma(\tau)$ in the evolution of QGP can also be found in Refs. [201,202].

Next, we present the above perturbative analytic solutions (34), (41) and the results for solving Eqs. (32) directly in a numerical way. We choose the $\tau_0 = 0.6$ fm/c and the speed of sound $c_s^2 = 1/3$. The electric conductivity σ are given by $\sigma \sim 5.8T/T_c$ MeV from lattice QCD [203–205] and $\sigma \sim 20$–30 MeV for $T \simeq 200$ MeV from the holographic QCD [13,15]. In this work, we choose the region of the initial electric conductivity σ_0 as $\sigma_0 \sim 5$–30 MeV$\simeq 0.025$–0.15 fm^{-1}.

From the solutions (41), the proper timescaled electric field $E/E_0 \times (\tau/\tau_0)$ and chiral density $n_5/n_{5,0} \times (\tau/\tau_0)$ will not be sensitive to the E_0^2/ε_0. We have also confirmed it numerically. For simplicity, we fix $E_0^2/\varepsilon_0 = 0.1$ for the discussion on $E/E_0 \times (\tau/\tau_0)$ and $n_5/n_{5,0} \times (\tau/\tau_0)$.

In the left-hand side of Fig. 1, we plot the proper timescaled electric field $E/E_0 \times (\tau/\tau_0)$ as functions of the proper time τ with different sets of parameters $a_{1,2}, \sigma_0$.

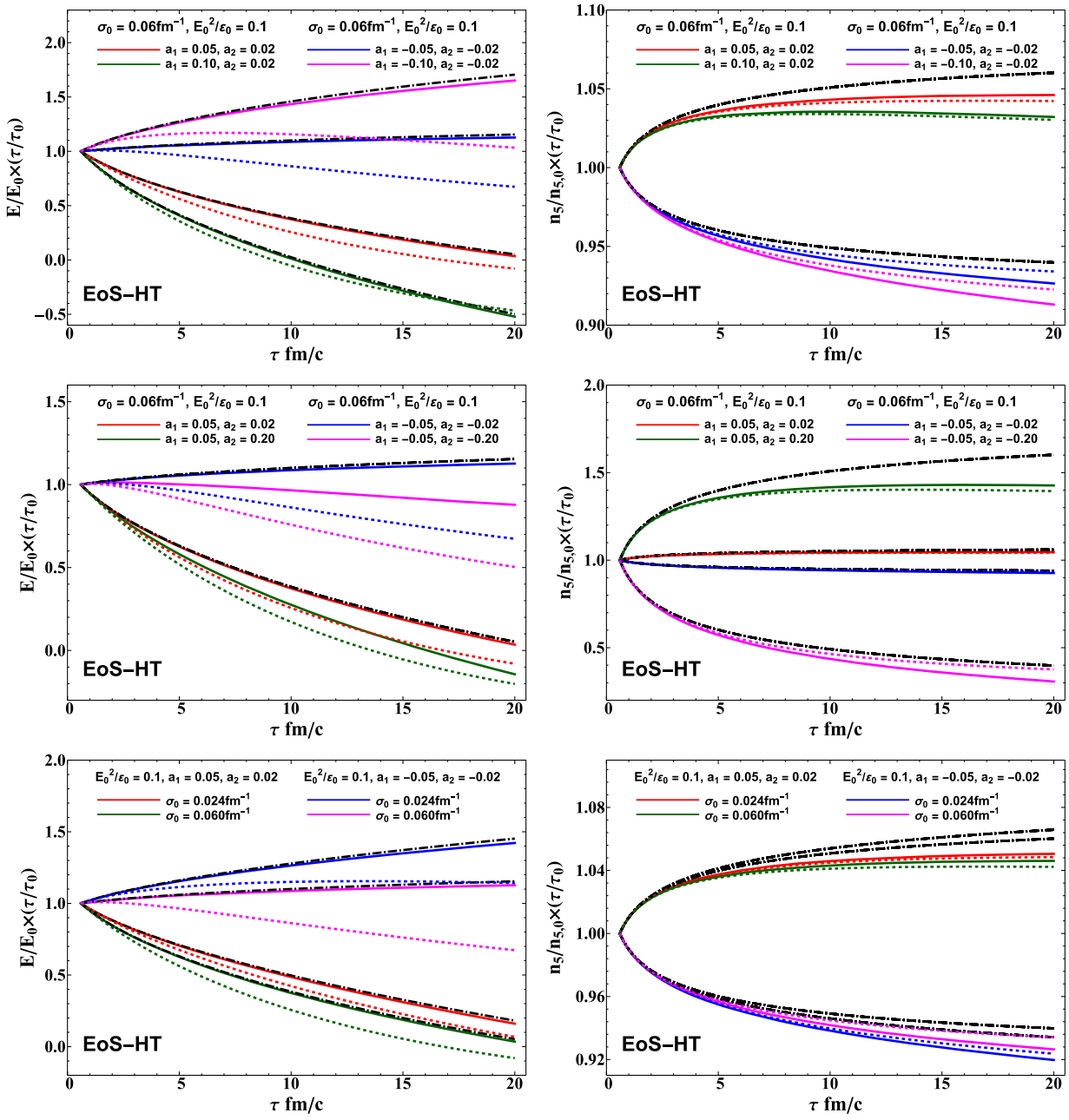

FIG. 1. The proper timescaled electric field $E/E_0 \times (\tau/\tau_0)$ and chiral charge density $n_5/n_{5,0} \times (\tau/\tau_0)$ computed with EoS-HT (14) as functions of proper time τ with different parameters a_1, a_2, σ_0. We have fixed $E_0^2/\varepsilon_0 = 0.1$. The colored solid, black dashed-dotted, and colored dotted lines denote the results for solving the results from Eqs. (32), (33) numerically, analytic solutions (34), (41) and numerical results with a constant σ derived in Refs. [162,163], respectively.

The analytic solutions (34), (41) agree with the numerical results well. Note that our analytic solutions (41) for E do not have the a_2 dependence and, therefore, it only matches the numerical results in small $|a_2|$ case.

Similar to Refs. [162,163], we find that $E(\tau)$ decays faster when a_1 increases and E/E_0 can be negative at late time on condition that the initial E and B field are of the same orientation due to the competition between the anomalous conservation equation and Maxwell's equations.

We can also compare our results (solid or dashed-dotted lines) with temperature dependent $\sigma(\tau)$ to those with a constant σ derived in Refs. [162,163] (dotted lines). From Eq. (44) in the order of $\hbar^0$, $E(\tau) \sim \frac{1}{\tau} e^{-\sigma_0 \tau_0^{c_s^2} \tau^{1-c_s^2}} \sim \frac{1}{\tau} e^{-\sigma_0 \tau_0^{1/3} \tau^{2/3}} \leq \frac{1}{\tau} e^{-\sigma_0 \tau_0}$ when $\tau \geq \tau_0$. It means that the $\sigma(\tau)$ will quicken up the decaying of $E(\tau)$. We can understand it in the following way. At late time limit, $\lim_{\tau\to\infty} \sigma(\tau) \to 0$, the fluid becomes dilute close to the vacuum and the EM

fields decays much rapidity in the vacuum than in a medium. It is consistent with the results in Fig. 1. On the other hand, we also notice that when $a_{1,2}$ are negative, the $E/E_0 \times (\tau/\tau_0)$ may increase when proper time grows. It corresponds to the cases that EM fields gain the energy from the medium.

In the right-hand side of Fig. 1, we present the proper timescaled chiral density $n_5/n_{5,0} \times (\tau/\tau_0)$ as functions of the proper time τ with different sets of parameters a_1, a_2 and σ_0. Since our analytic solutions (41) for n_5 do not have the a_1 dependence, the analytic solutions for n_5 agree with the numerical results in small $|a_1|$ limit. We find that the proper timescaled chiral density computed from numerical solutions is not sensitive to the a_1 and σ_0 at early proper time. It agrees with the analytic solutions (41). At late proper time, proper time scaled chiral density computed from numerical solutions decreases with a_1 decreasing. We also observe that the proper timescaled chiral density computed from numerical solutions increases when a_2 grows. The temperature dependent $\sigma(\tau)$ seems not to affect the evolution of n_5, which can also be found in the solutions (41).

In Figs. 2, we plot the proper timescaled energy density $\varepsilon/\varepsilon_0 \times (\tau/\tau_0)^{1+c_s^2}$ as functions of the proper time τ with different sets of parameters a_1, a_2, σ_0 and E_0^2/ε_0.

As shown in Eqs. (41), our analytic solutions for ε do not have a_2 dependence and it only corresponds to the small $|a_2|$ limit. On the other hand, we observe that our analytic solutions (41) for ε matches the numerical results only at early proper time. It implies that the system is beyond the approximation for ε in Eq. (36) at late proper time.

We observe that the proper timescaled energy density increases when $a_1, a_2, \sigma_0, E_0^2/\varepsilon_0$ increases. When a_1, a_2, $\sigma_0, E_0^2/\varepsilon_0$ is large enough, the proper timescaled energy density can increase with proper time. It corresponds that the medium gains the energy from the EM fields, which is also found in the ideal MHD with a background magnetic field [158,159]. In the comparison with the case of constant σ_0, we find that the temperature dependent $\sigma(\tau)$ enhances the decaying of energy density.

In this section, we have solved the MHD with the temperature dependent $\sigma(\tau)$ in Eq. (15) and EoS-HT (14). We present both the analytic solutions (41) up to the $\mathcal{O}(\hbar)$ and the numerical results.

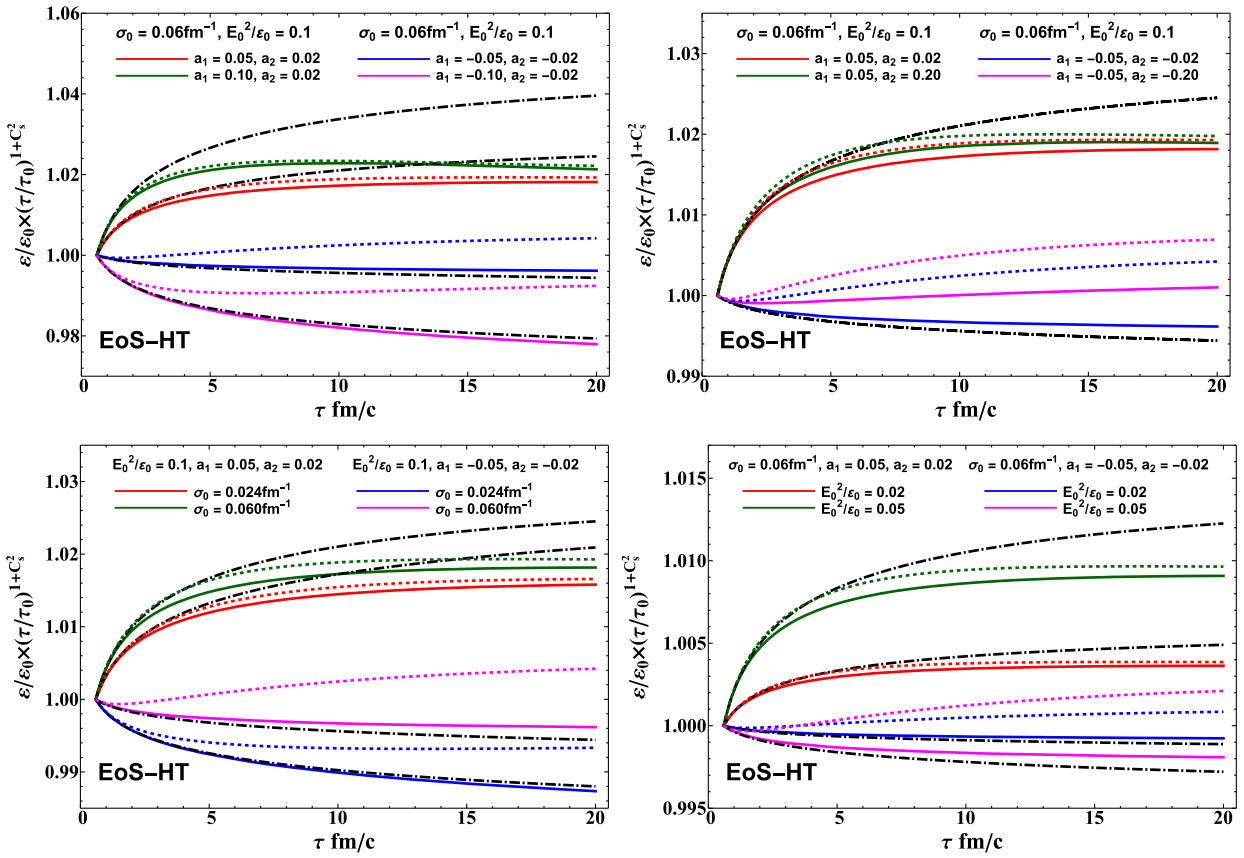

FIG. 2. The proper timescaled energy density $\varepsilon/\varepsilon_0 \times (\tau/\tau_0)^{1+c_s^2}$ computed with EoS-HT (14) as functions of proper time τ with different parameters a_1, a_2, σ_0 and E_0^2/ε_0. The colored solid, black dashed-dotted, and colored dotted lines denote the results for solving the results from Eqs. (32), (33) numerically, analytic solutions (34), (41) and numerical results with a constant σ derived in Refs. [162,163], respectively.

V. SOLUTIONS IN HIGH CHIRAL CHEMICAL POTENTIAL LIMIT

In this section, we solve the simplified differential equations (26), (27) with the EoS-HC (16) and temperature and energy density dependent conductivity (17).

Following the same method in the previous section, we can get the Eqs. (32), (33), (34), (35). The conductivity (17) becomes,

$$\sigma = \sigma_0 \left(\frac{\tau_0}{\tau}\right)^{\frac{2}{3}-c_s^2} y^{2/3} \cdot z^{-c_s^2/(1+c_s^2)}. \tag{46}$$

Using variables x, y, z, Eqs. (33) becomes,

$$\begin{aligned}
\frac{d}{d\tau}x &= -\sigma_0 \left(\frac{\tau_0}{\tau}\right)^{\frac{2}{3}-c_s^2} x y^{2/3} \cdot z^{-c_s^2/(1+c_s^2)} - \frac{a_1'}{\tau_0}\left(\frac{\tau_0}{\tau}\right)^{1/3} y^{1/3}, \\
\frac{d}{d\tau}y &= a_2' \frac{x}{\tau}, \\
\frac{d}{d\tau}z &= \frac{E_0^2}{\varepsilon_0}\sigma_0 \left(\frac{\tau_0}{\tau}\right)^{\frac{5}{3}-2c_s^2} x^2 y^{2/3} z^{-c_s^2/(1+c_s^2)} + \frac{a_1'}{\tau_0}\left(\frac{E_0^2}{\varepsilon_0}\right)\left(\frac{\tau_0}{\tau}\right)^{\frac{4}{3}-c_s^2} x y^{1/3},
\end{aligned} \tag{47}$$

where $x(\tau_0) = y(\tau_0) = z(\tau_0) = 1$, and dimensionless constants a_1', a_2' read

$$\begin{aligned}
a_1' &= eC\chi \left(\frac{n_{5,0}}{a}\right)^{1/3} \frac{B_0}{E_0}\tau_0, \\
a_2' &= e^2 C\chi \frac{E_0 B_0}{n_{5,0}}\tau_0.
\end{aligned} \tag{48}$$

We follow the same power counting in Sec. IV, i.e., $\mathcal{O}(\frac{E_0^2}{\varepsilon_0}) \sim \mathcal{O}(a_{1,2}') \sim \mathcal{O}(\hbar)$ and derive the analytic solutions up to the order of $\hbar$,

$$\begin{aligned}
x(\tau) &= e^{m_1'(\tilde{\tau}'-1)} + \frac{3}{2}a_1 e^{m_1'\tilde{\tau}'}(n_1'-1)[\mathcal{E}(n_1', m_1') - \tilde{\tau}'^{2/(1+3c_s^2)}\mathcal{E}(n_1', m_1'\tilde{\tau}')], \\
y(\tau) &= 1 - \frac{3}{2}a_2 e^{-m_1'}(n_1'-1)[\mathcal{E}(1, -m_1') - \mathcal{E}(1, -m_1'\tilde{\tau}')], \\
z(\tau) &= 1 - m_1'\frac{E_0^2}{\varepsilon_0}e^{-2m_1'}[\mathcal{E}(-2n_1'+1, -2m_1') - \tilde{\tau}'^{2n_1'}\mathcal{E}(-2n_1'+1, -2m_1'\tilde{\tau}')] \\
&\quad - \frac{3}{2}a_1\left(\frac{E_0^2}{\varepsilon_0}\right)e^{-m_1'}(n_1'-1)[\mathcal{E}(-n_1'+1, -m_1') - \tilde{\tau}'^{n_1'}\mathcal{E}(-n_1'+1, -m_1'\tilde{\tau}')],
\end{aligned} \tag{49}$$

where we introduce

$$\begin{aligned}
n_1' &= \frac{-1+3c_s^2}{1+3c_s^2}, \\
m_1' &= -\frac{\sigma_0\tau_0}{\frac{1}{3}+c_s^2}, \\
\tilde{\tau}' &= \left(\frac{\tau_0}{\tau}\right)^{-\frac{1}{3}-c_s^2}.
\end{aligned} \tag{50}$$

For the numerical calculations, we choose the $\tau_0 = 0.6$ fm/c and the speed of sound $c_s^2 = 1/3$. Meanwhile, we fix $E_0^2/\varepsilon_0 = 0.1$ for the discussion on $E/E_0 \times (\tau/\tau_0)$ and $n_5/n_{5,0} \times (\tau/\tau_0)$ again.

In Figs. 3, we plot the proper timescaled electric field $E/E_0 \times (\tau/\tau_0)$, chiral density $n_5/n_{5,0} \times (\tau/\tau_0)$ as functions of the proper time τ with different parameters a_1', a_2' and σ_0. Interesting, in the comparison with Fig. 1, the proper timescaled electric field in small $|a_2'|$ cases and chiral density, computed with EoS-HC, seem to be close the those computed with EoS-HT when we choose $a_1 = a_1'$ and $a_2 = a_2'$. It means that the evolution of electric fields in the small $|a_2'|$ cases and chiral density are not sensitive to the EoS.

Different to the constant electric conductivity case in Refs. [162,163] (colored dotted e/bclines in Fig. 3), the temperature and energy density dependent $\sigma(\tau)$ with

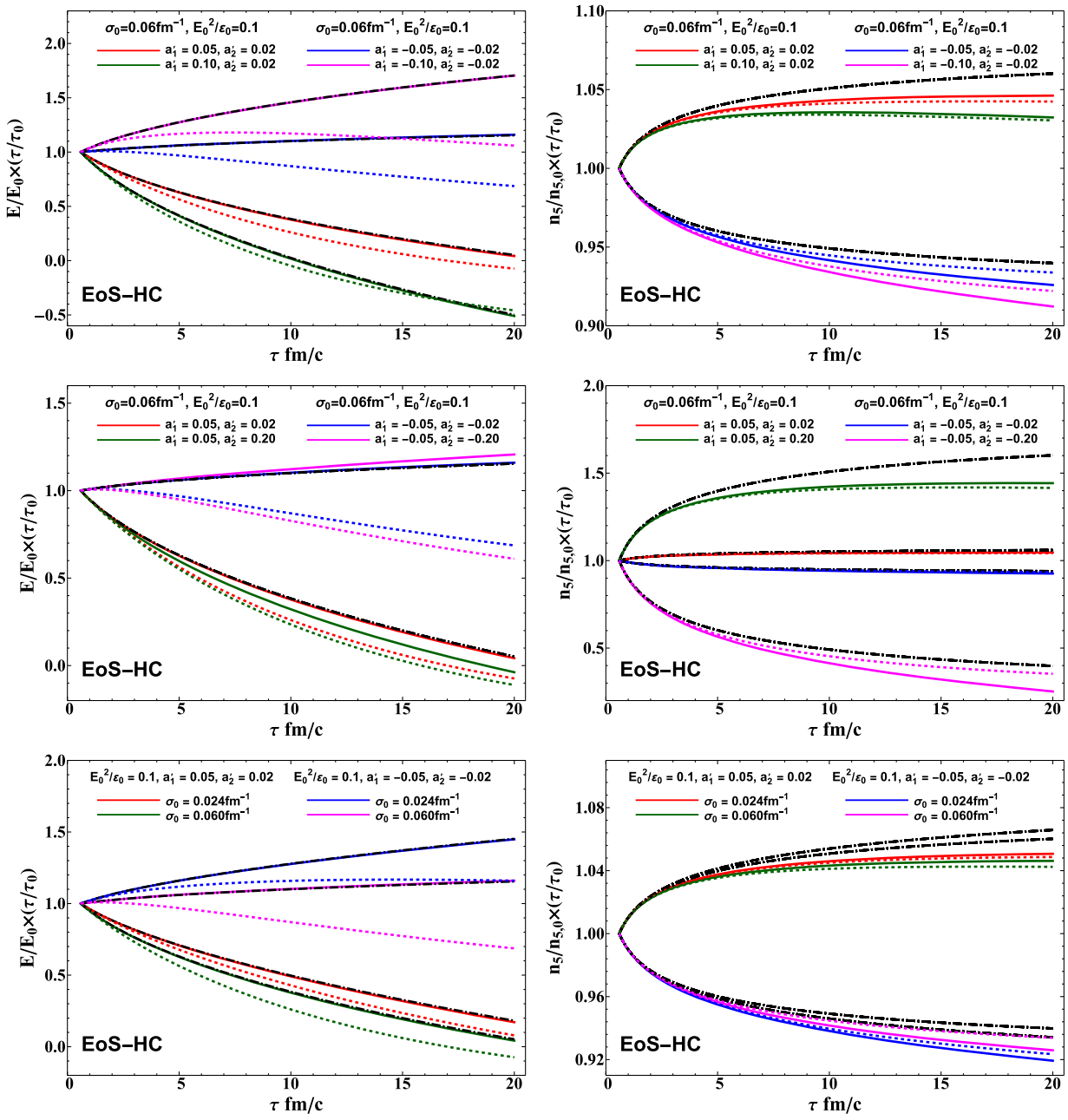

FIG. 3. The proper timescaled electric field $E/E_0 \times (\tau/\tau_0)$ and chiral density $n_5/n_{5,0} \times (\tau/\tau_0)$ computed with EoS-HC (16) as functions of proper time τ with different parameters a_1, a_2, σ_0. For simplicity, we fix $E_0^2/\varepsilon_0 = 0.1$. The colored solid, black dashed-dotted, and colored dotted lines denote the results for solving the results from Eqs. (32), (33) numerically, analytic solutions (34), (49) and numerical results with a constant σ derived in Refs. [162,163], respectively.

EoS-HC will slow down the decaying of electric fields when $a_2' < 0$. Such behavior is also also insensitive to the $|a_2'|$ when $a_2' < 0$.

In Fig. 4, we present the proper timescaled energy density $\varepsilon/\varepsilon_0 \times (\tau/\tau_0)^{1+c_s^2}$ as functions of the proper time τ with different parameters a_1', a_2', σ_0 and E_0^2/ε_0. We observe the similarity in small $|a_2'|$ cases between the figures in Fig. 4 and in Fig. 2. When $a_2' < 0$, the evolution of energy density is insensitive to the $|a_2'|$. The temperature and energy density dependent electric conductivity $\sigma(\tau)$ will accelerate the decaying of energy density when $a_2' < 0$. Combining with the results in Fig. 3, it implies that the temperature and energy density dependent electric conductivity $\sigma(\tau)$ helps the electric fields gain the energy from the medium.

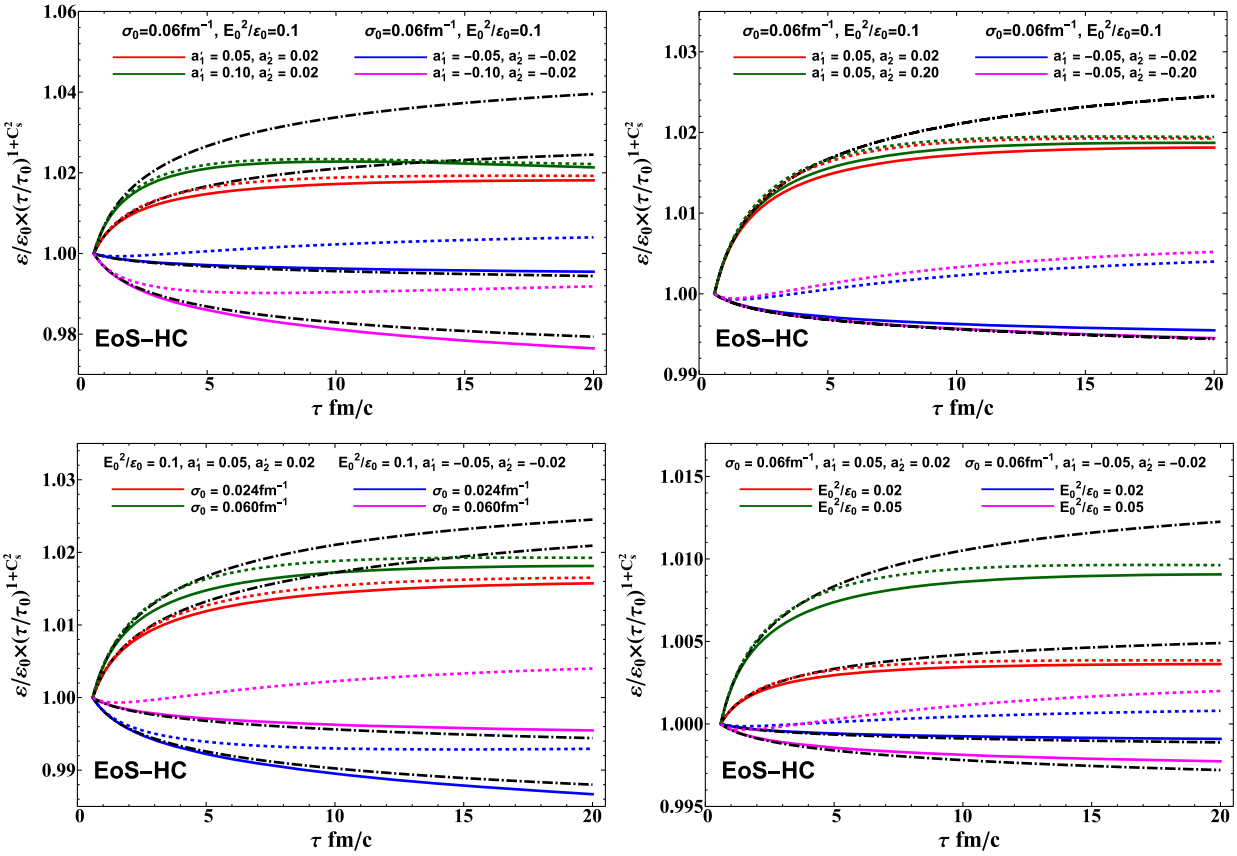

FIG. 4. The proper timescaled energy density $\varepsilon/\varepsilon_0 \times (\tau/\tau_0)^{1+c_s^2}$ computed with EoS-HC (16) as functions of proper time τ with different parameters a_1, a_2, σ_0 and E_0^2/ε_0. The colored solid, black dashed-dotted and colored dotted lines denote the results for solving the results from Eqs. (32), (33) numerically, analytic solutions (34), (49) and numerical results with a constant σ derived in Refs. [162,163], respectively.

In this section, we have solved the MHD with the temperature and energy density dependent $\sigma(\tau)$ in Eq. (17) and EoS-HC. We present both the analytic solutions (49) up to the $\mathcal{O}(\hbar)$ and the numerical results.

VI. SPLITTING OF GLOBAL POLARIZATION FOR Λ AND $\bar{\Lambda}$ HYPERONS INDUCED BY MAGNETIC FIELDS

In Sec. IV and V, we have derived the analytic and numerical solutions for the relativistic MHD in a Bjorken expansion with the transverse EM fields and a temperature dependent electric conductivity. In this section, we implement the results for relativistic MHD to the global polarization of Λ and $\bar{\Lambda}$ hyperons in the relativistic heavy ion collisions. We will first review the general theoretical framework for the global polarization of Λ and $\bar{\Lambda}$ hyperons in the relativistic heavy ion collisions. We will show that the magnetic fields can induce the splitting of global polarization of Λ and $\bar{\Lambda}$ hyperons. Then, we implement our solutions for the magnetic fields to estimate the splitting effects at different collisional energies and compare the results with experimental data.

The polarization pesudovector is given by the modified Cooper-Frye formula [217,218],

$$\mathcal{S}^\mu(\mathbf{p}) = \frac{\int d\Sigma \cdot p \mathcal{J}_5^\mu(p,X)}{2m_\Lambda \int d\Sigma \cdot \mathcal{N}(p,X)}, \tag{51}$$

where m_Λ is the mass of Λ hyperon, Σ is the freeze out hypersurface, $\mathcal{J}_5^\mu(p,X)$ and $\mathcal{N}^\mu(p,x)$ are axial and vector components of Wigner functions in phase space. By inserting the general solutions in Wigner functions [36,38,45,47,50,72,73], the polarization vector $\mathcal{S}^\mu$ in Eq. (51) can be divide as several different parts [47,118,119],

$$\begin{aligned}\mathcal{S}^\mu(\mathbf{p}) = {} & \mathcal{S}^\mu_{\text{thermal}}(\mathbf{p}) + \mathcal{S}^\mu_{\text{shear}}(\mathbf{p}) + \mathcal{S}^\mu_{\text{accT}}(\mathbf{p}) \\ & + \mathcal{S}^\mu_{\text{chemical}}(\mathbf{p}) + \mathcal{S}^\mu_{\text{EB}}(\mathbf{p}),\end{aligned} \tag{52}$$

where

$$\mathcal{S}^{\mu}_{\text{thermal}}(\mathbf{p}) = \int d\Sigma^{\sigma} F_{\sigma} \epsilon^{\mu\nu\alpha\beta} p_{\nu} \partial_{\alpha} \frac{u_{\beta}}{T},$$
$$\mathcal{S}^{\mu}_{\text{shear}}(\mathbf{p}) = \int d\Sigma^{\sigma} F_{\sigma} \frac{\epsilon^{\mu\nu\alpha\beta} p_{\nu} u_{\beta}}{(u\cdot p)T} \times p^{\rho}[\partial_{\rho} u_{\alpha} + \partial_{\alpha} u_{\rho} - u_{\rho}(u\cdot\partial)u_{\alpha}],$$
$$\mathcal{S}^{\mu}_{\text{accT}}(\mathbf{p}) = -\int d\Sigma^{\sigma} F_{\sigma} \frac{\epsilon^{\mu\nu\alpha\beta} p_{\nu} u_{\alpha}}{T} \left[(u\cdot\partial)u_{\beta} - \frac{\partial_{\beta} T}{T}\right],$$
$$\mathcal{S}^{\mu}_{\text{chemical}}(\mathbf{p}) = 2\int d\Sigma^{\sigma} F_{\sigma} \frac{1}{(u\cdot p)} \epsilon^{\mu\nu\alpha\beta} p_{\alpha} u_{\beta} \partial_{\nu} \frac{\mu_B}{T},$$
$$\mathcal{S}^{\mu}_{\text{EB}}(\mathbf{p}) = 2\int d\Sigma^{\sigma} F_{\sigma} \left[\frac{\epsilon^{\mu\nu\alpha\beta} p_{\alpha} u_{\beta} E_{\nu}}{(u\cdot p)T} + \frac{B^{\mu}}{T}\right], \tag{53}$$

with

$$F^{\mu} = \frac{\hbar}{8 m_{\Lambda} \Phi(\mathbf{p})} p^{\mu} f_{\text{eq}}(1 - f_{\text{eq}}),$$
$$\Phi(\mathbf{p}) = \int d\Sigma^{\mu} p_{\mu} f_{\text{eq}}. \tag{54}$$

where $\Phi(\mathbf{p}) = \int d\Sigma^{\mu} p_{\mu} f_{\text{eq}}(x,p)$ is the particle number density at freeze out hypersurface, μ_B is the baryon chemical potential and f_{eq} is assumed as the standard Fermi-Dirac distribution function. The $\mathcal{S}^{\mu}_{\text{thermal}}(\mathbf{p}), \mathcal{S}^{\mu}_{\text{shear}}(\mathbf{p}), \mathcal{S}^{\mu}_{\text{accT}}(\mathbf{p})$ for Λ hyperons are the same as those for $\bar{\Lambda}$ hyperons. While, due to the difference in charge and baryon number, $\mathcal{S}^{\mu}_{\text{chemical}}(\mathbf{p})$ and $\mathcal{S}^{\mu}_{\text{EB}}(\mathbf{p})$ flip their sign when we change Λ to $\bar{\Lambda}$ hyperons. Therefore, the gradient of μ_B/T and EM fields can lead to the splitting of global polarization for Λ and $\bar{\Lambda}$ hyperons. An alternative mechanism induced by the interplay between chiral and helical vortical effects, without the incorporation of a magnetic field can also explain the difference in the global spin polarization of Λ and $\bar{\Lambda}$ hyperons [219–221].

In order to compare with experiments, we need to transform the polarization pseudovector in the rest frame of Λ and $\bar{\Lambda}$, named $\vec{P}^{*}(\mathbf{p})$

$$\vec{P}^{*}(\mathbf{p}) = \vec{P}(\mathbf{p}) - \frac{\vec{P}(\mathbf{p})\cdot\vec{p}}{p^{0}(p^{0}+m)}\vec{p}, \tag{55}$$

where

$$P^{\mu}(\mathbf{p}) \equiv \frac{1}{s}\mathcal{S}^{\mu}(\mathbf{p}), \tag{56}$$

with $s = 1/2$ being the spin of the particle. Finally, the local polarization is given by the averaging over momentum and rapidity as follows,

$$\langle \vec{P}(\phi_p) \rangle = \frac{\int_{y_{\min}}^{y_{\max}} dy \int_{p_{T\min}}^{p_{T\max}} p_T dp_T [\Phi(\mathbf{p})\vec{P}^{*}(\mathbf{p})]}{\int_{y_{\min}}^{y_{\max}} dy \int_{p_{T\min}}^{p_{T\max}} p_T dp_T \Phi(\mathbf{p})}, \tag{57}$$

where ϕ_p is the azimuthal angle.

In this work, we concentrate on the splitting induced by the magnetic fields. From Eq. (53), we introduce

$$\Delta\mathcal{P} = \mathcal{P}_{\Lambda} - \mathcal{P}_{\bar{\Lambda}}, \tag{58}$$

where $\mathcal{P}_{\Lambda}$ and $\mathcal{P}_{\bar{\Lambda}}$ are the integration of local polarization (57) alone the out-of-plane direction over the ϕ_p. Taking $1 - f_{\text{eq}} \simeq 1$ in Eqs. (53), the $\Delta\mathcal{P}$ induced by the magnetic fields is given by, $\Delta\mathcal{P}_{\text{EB}} \propto B^{y}/(m_{\Lambda}T)$. Recalling the definition spin magnetic moment, following Ref. [120], $\Delta\mathcal{P}$ induced by magnetic fields is estimated as

$$\Delta\mathcal{P}_{\text{EB}} \approx 2\frac{\mu_{\Lambda}}{T}\bar{B}, \tag{59}$$

where $\mu_{\Lambda} = -0.613\mu_N$ is the spin magnetic moment for Λ hyperons. In the Ref. [120], $\bar{B}$ is averaged the magnetic field. Also see other related theoretical studies on the splitting of polarization induced by EM fields [121–123].

Next, we will evaluate the $\Delta\mathcal{P}_{\text{EB}}$ in the framework of relativistic MHD. Recalling the expression in Eq. (57), since the polarization pseudovector is computed near the freeze out surface, we need to know the averaged magnetic fields at the freeze out hypersurface.

For the initial magnetic fields, we choose the maximum value of space-averaged initial magnetic fields in different impact parameters, which is computed by Ref. [222]. The initial proper time is chosen as $\tau_0 \simeq 0.6$ fm/c.

The evolution of the EM field can be estimated by using our solutions in Secs. IV and V. In the ideal MHD limit of Eq (28), B^{y} dominates in the lab frame [158–161]. While the temperature dependent electric conductivity will turn on the B^{x} in the lab frame. For simplicity, as a first attempt, we first estimate the magnetic fields in ideal MHD limit and we will comment on the effects of temperature dependent conductivity at the end of this section. Physically, it is also natural to choose the $B^{y}(\tau_f)$ with τ_f being the proper time for the chemical freeze out instead of the averaged $\bar{B}$.

For simplicity, we choose the $\tau_f = 10$ fm/c for all collision energies. The temperature for the chemical freeze out is followed by the experimental studies in Ref. [223]. We summarize these parameters in different collision energies in Table I.

In Fig. 5, we plot the splitting of the global polarization for Λ and $\bar{\Lambda}$ hyperons, and compare our estimation from Eq. (59) with the data from STAR measurements [99,224] at $\sqrt{s_{NN}} = 7.7, 11.5, 27, 39, 62.4, 200$ GeV collisions. We find that the $\Delta\mathcal{P}_{\text{EB}}$ computed from our framework agrees with the data expect the results at $\sqrt{s_{NN}} = 7.7$ GeV. Roughly speaking, in the high energy collisions, the quark pairs are generated from the vacuum and therefore, the net

TABLE I. Collision energies, temperature given by Ref. [223], the initial space-averaged magnetic fields from Ref. [222], the magnetic fields estimated by Eq. (31) with $\tau_f = 10$ fm/c.

$\sqrt{s_{NN}}$ (GeV)	7.7	11.5	27	39	62.4	200
T (MeV)	144.3	149.4	155.0	156.4	160.3	164.3
space-averaged $eB(\tau_0)/m_\pi^2$	9.1×10^{-2}	1.7×10^{-1}	4.5×10^{-1}	4.5×10^{-1}	3.2×10^{-1}	5.6×10^{-2}
$eB(\tau_f)/m_\pi^2$	5.5×10^{-3}	1.0×10^{-2}	2.7×10^{-2}	2.7×10^{-2}	1.9×10^{-2}	3.3×10^{-3}

baryon number and baryon chemical potential are approximately vanishing. The splitting induced by EM fields may dominate in the global polarization of Λ and $\bar{\Lambda}$ hyperons in the high energy region. On the other hand, the collisions in the low energy region, the net baryon density is not negligible and will play a crucial role to the global and local polarization, e.g., see Ref. [109] and the discussions on the simulations for spin Hall effects in heavy ion collisions [110,124]. Our results indicates that the magnetic fields may be not strong enough to cause such huge splitting of global polarization in low energy region. It implies that the contributions from $\nabla\mu_B/T$ [109,110] or the interplay between chiral and helical vortical effects [219–221] may dominate the splitting of global polarization in low energy collisions.

Before concluding this section, we address the impact of temperature dependent electric conductivity on the electromagnetic field. As previously mentioned, the temperature dependence of the electric conductivity leads to the generation of a magnetic field component, B^x, in the lab frame. This magnetic field can ultimately alter the averaged magnetic fields at the freezeout hypersurface. However, due to the significant experimental uncertainties and the fact that our calculation of the magnetic field decay in the ideal MHD limit agrees with experimental data, except for collisions at $\sqrt{s_{NN}} = 7.7$ GeV, we think that we currently do not need to consider the temperature dependent electric conductivity in the context of splitting of global polarization.

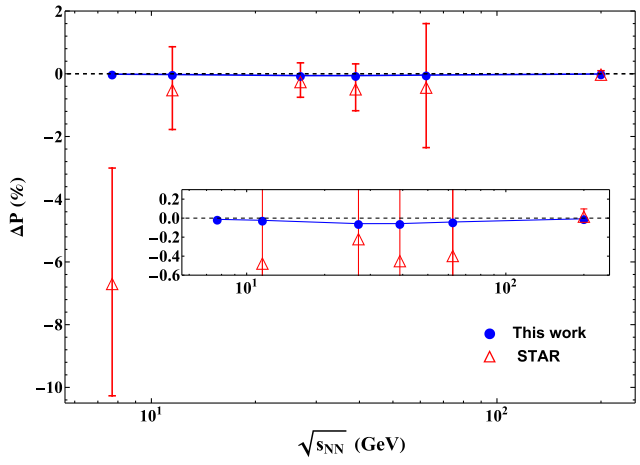

FIG. 5. The difference of the global polarization between Λ and $\bar{\Lambda}$ hyperons in different collision energies. The triangle points are derived from STAR measurements [99,224]. The filled circle points denotes the estimation from Eqs. (59) where the initial magnetic fields at $\tau_0 = 0.6$ fm/c are given by Ref. [222] and the evolution of magnetic fields are given by Eq. (31) with final time $\tau_f = 10$ fm/c.

VII. SUMMARY

We have derived the solutions of the relativistic anomalous magnetohydronamic with longitudinal Bjorken boost invariance and transverse electromagnetic fields in the presence of temperature or energy density dependent electric conductivity.

After a short review on the anomalous MHD in Sec. II, we simplify the energy-momentum and charge currents conversation equations coupled to the Maxwell's equations. To close the system, we introduce two kinds of EoS, i.e., EoS-HT (14) and EoS-HC (16) correspond to the high temperature and high chiral chemical potential limits, respectively. The electric conductivity is also parametrized as Eqs. (15) and (17) for the EoS-HT and EoS-HC, respectively. We assume that the initial conditions for the system is a Bjorken velocity (24) with initial EM fields in Eq. (25). After some calculations, we confirm that the Bjorken boost invariance holds during the evolution. The main differential equations reduce to Eqs. (26), (27).

Next, in Sec. III, we derive the perturbative analytic solutions (34), (41) up to the order of $\hbar$ for the simplified differential equations (26), (27) with the EoS-HT (14) and temperature dependent conductivity (15). We present the numerical solutions for electric fields, chiral density and energy density in Figs. 1, 2. We find that the temperature dependent $\sigma(\tau)$ will quicken up the decaying of electric fields. While, the decaying of chiral density seems not to be sensitive to the $\sigma(\tau)$.

Similarly, we derive the perturbative analytic solutions (34), (49) up to the order of $\hbar$ with the EoS-HC (16) and temperature dependent conductivity (17). The numerical results for the proper timescaled electric fields, chiral density and energy density are shown in Figs. 3, 4. We find that the decaying of electric fields and energy density in the small $|a_2'|$ limit and chiral density seem not be affected by the EoS when we choose $a_1 = a_1'$ and $a_2 = a_2'$. On the other hand, when $a_2' < 0$, temperature and energy density dependent electric conductivity $\sigma(\tau)$ will slow down or accelerate the decaying of electric fields or energy density, respectively.

At last, we implement the results for relativistic MHD to the global polarization of Λ and $\bar{\Lambda}$ hyperons in the relativistic heavy ion collisions in Sec. VI. The splitting of global polarization for Λ and $\bar{\Lambda}$ hyperons is estimated by Eq. (59). In Fig. 5, we plot the splitting of the global polarization for Λ and $\bar{\Lambda}$ hyperons, and compare our estimation from Eq. (59) with the data from STAR measurements at $\sqrt{s_{NN}} = 7.7, 11.5, 27, 39, 62.4, 200$ GeV collisions. The $\Delta\mathcal{P}_{\mathrm{EB}}$ computed from our framework agrees with the data in both high and intermediate collisions energies and fails at $\sqrt{s_{NN}} = 7.7$ GeV. It implies that the contributions from other sources may dominate the splitting of global polarization in low energy collisions.

ACKNOWLEDGMENTS

The authors would like to thank Qun Wang and Maxim Chernodub for helpful discussion. This work is supported in part by the National Key Research and Development Program of China under Contract No. 2022YFA1605500 and National Natural Science Foundation of China (NSFC) under Grants No. 12075235 and No. 12135011.

[1] V. Skokov, A. Y. Illarionov, and V. Toneev, Int. J. Mod. Phys. A **24**, 5925 (2009).
[2] A. Bzdak and V. Skokov, Phys. Lett. B **710**, 171 (2012).
[3] W.-T. Deng and X.-G. Huang, Phys. Rev. C **85**, 044907 (2012).
[4] V. Roy and S. Pu, Phys. Rev. C **92**, 064902 (2015).
[5] A. Vilenkin, Phys. Rev. D **22**, 3080 (1980).
[6] D. Kharzeev and A. Zhitnitsky, Nucl. Phys. **A797**, 67 (2007).
[7] D. E. Kharzeev, L. D. McLerran, and H. J. Warringa, Nucl. Phys. **A803**, 227 (2008).
[8] K. Fukushima, D. E. Kharzeev, and H. J. Warringa, Phys. Rev. D **78**, 074033 (2008).
[9] Y. Aghababaie and C. P. Burgess, Phys. Rev. D **70**, 085003 (2004).
[10] D. E. Kharzeev and H.-U. Yee, Phys. Rev. D **83**, 085007 (2011).
[11] Y. Burnier, D. E. Kharzeev, J. Liao, and H.-U. Yee, Phys. Rev. Lett. **107**, 052303 (2011).
[12] X.-G. Huang and J. Liao, Phys. Rev. Lett. **110**, 232302 (2013).
[13] S. Pu, S.-Y. Wu, and D.-L. Yang, Phys. Rev. D **89**, 085024 (2014).
[14] Y. Jiang, X.-G. Huang, and J. Liao, Phys. Rev. D **91**, 045001 (2015).
[15] S. Pu, S.-Y. Wu, and D.-L. Yang, Phys. Rev. D **91**, 025011 (2015).
[16] J.-W. Chen, T. Ishii, S. Pu, and N. Yamamoto, Phys. Rev. D **93**, 125023 (2016).
[17] E. V. Gorbar, I. A. Shovkovy, S. Vilchinskii, I. Rudenok, A. Boyarsky, and O. Ruchayskiy, Phys. Rev. D **93**, 105028 (2016).
[18] E. V. Gorbar, V. A. Miransky, I. A. Shovkovy, and P. O. Sukhachov, Phys. Rev. B **95**, 115202 (2017).
[19] E. V. Gorbar, V. A. Miransky, I. A. Shovkovy, and P. O. Sukhachov, Phys. Rev. Lett. **118**, 127601 (2017).
[20] E. V. Gorbar, V. A. Miransky, I. A. Shovkovy, and P. O. Sukhachov, Phys. Rev. B **95**, 205141 (2017).
[21] K. Fukushima, D. E. Kharzeev, and H. J. Warringa, Phys. Rev. Lett. **104**, 212001 (2010).
[22] H. J. Warringa, Phys. Rev. D **86**, 085029 (2012).
[23] P. Copinger, K. Fukushima, and S. Pu, Phys. Rev. Lett. **121**, 261602 (2018).
[24] P. Copinger and S. Pu, Int. J. Mod. Phys. A **35**, 2030015 (2020).
[25] P. Copinger and S. Pu, Phys. Rev. D **105**, 116014 (2022).
[26] D. E. Kharzeev, K. Landsteiner, A. Schmitt, and H.-U. Yee, Lect. Notes Phys. **871**, 1 (2013).
[27] D. E. Kharzeev, J. Liao, S. A. Voloshin, and G. Wang, Prog. Part. Nucl. Phys. **88**, 1 (2016).
[28] J. Liao, Pramana **84**, 901 (2015).
[29] V. A. Miransky and I. A. Shovkovy, Phys. Rep. **576**, 1 (2015).
[30] X.-G. Huang, Rep. Prog. Phys. **79**, 076302 (2016).
[31] K. Fukushima, Prog. Part. Nucl. Phys. **107**, 167 (2019).
[32] A. Bzdak, S. Esumi, V. Koch, J. Liao, M. Stephanov, and N. Xu, Phys. Rep. **853**, 1 (2020).
[33] J. Zhao and F. Wang, Prog. Part. Nucl. Phys. **107**, 200 (2019).
[34] J.-H. Gao, G.-L. Ma, S. Pu, and Q. Wang, Nucl. Sci. Tech. **31**, 90 (2020).
[35] I. A. Shovkovy, arXiv:2111.11416.
[36] J.-H. Gao, Z.-T. Liang, S. Pu, Q. Wang, and X.-N. Wang, Phys. Rev. Lett. **109**, 232301 (2012).
[37] D. T. Son and N. Yamamoto, Phys. Rev. D **87**, 085016 (2013).
[38] J.-W. Chen, S. Pu, Q. Wang, and X.-N. Wang, Phys. Rev. Lett. **110**, 262301 (2013).
[39] M. A. Stephanov and Y. Yin, Phys. Rev. Lett. **109**, 162001 (2012).
[40] C. Manuel and J. M. Torres-Rincon, Phys. Rev. D **89**, 096002 (2014).
[41] J.-W. Chen, J.-H. Gao, J. Liu, S. Pu, and Q. Wang, Phys. Rev. D **88**, 074003 (2013).
[42] C. Manuel and J. M. Torres-Rincon, Phys. Rev. D **90**, 076007 (2014).
[43] J.-Y. Chen, D. T. Son, M. A. Stephanov, H.-U. Yee, and Y. Yin, Phys. Rev. Lett. **113**, 182302 (2014).
[44] J.-Y. Chen, D. T. Son, and M. A. Stephanov, Phys. Rev. Lett. **115**, 021601 (2015).
[45] Y. Hidaka, S. Pu, and D.-L. Yang, Phys. Rev. D **95**, 091901 (2017).

[46] N. Mueller and R. Venugopalan, Phys. Rev. D **97**, 051901 (2018).
[47] Y. Hidaka, S. Pu, and D.-L. Yang, Phys. Rev. D **97**, 016004 (2018).
[48] J.-h. Gao, S. Pu, and Q. Wang, Phys. Rev. D **96**, 016002 (2017).
[49] Y.-C. Liu, L.-L. Gao, K. Mameda, and X.-G. Huang, Phys. Rev. D **99**, 085014 (2019).
[50] Y. Hidaka and D.-L. Yang, Phys. Rev. D **98**, 016012 (2018).
[51] A. Huang, S. Shi, Y. Jiang, J. Liao, and P. Zhuang, Phys. Rev. D **98**, 036010 (2018).
[52] Y. Hidaka, S. Pu, and D.-L. Yang, Nucl. Phys. **A982**, 547 (2019).
[53] J.-H. Gao, Z.-T. Liang, Q. Wang, and X.-N. Wang, Phys. Rev. D **98**, 036019 (2018).
[54] J.-H. Gao and Z.-T. Liang, Phys. Rev. D **100**, 056021 (2019).
[55] Z. Wang, X. Guo, S. Shi, and P. Zhuang, Phys. Rev. D **100**, 014015 (2019).
[56] S. Li and H.-U. Yee, Phys. Rev. D **100**, 056022 (2019).
[57] N. Weickgenannt, X.-L. Sheng, E. Speranza, Q. Wang, and D. H. Rischke, Phys. Rev. D **100**, 056018 (2019).
[58] K. Hattori, Y. Hidaka, and D.-L. Yang, Phys. Rev. D **100**, 096011 (2019).
[59] S. Lin and A. Shukla, J. High Energy Phys. 06 (2019) 060.
[60] S. Lin and L. Yang, Phys. Rev. D **101**, 034006 (2020).
[61] J.-H. Gao, Z.-T. Liang, and Q. Wang, Phys. Rev. D **101**, 096015 (2020).
[62] N. Weickgenannt, E. Speranza, X.-l. Sheng, Q. Wang, and D. H. Rischke, Phys. Rev. Lett. **127**, 052301 (2021).
[63] N. Weickgenannt, X.-L. Sheng, E. Speranza, Q. Wang, and D. H. Rischke, Nucl. Phys. **A1005**, 121963 (2021).
[64] Y.-C. Liu, K. Mameda, and X.-G. Huang, Chin. Phys. C **44**, 094101 (2020); **45**, 089001(E) (2021).
[65] A. Huang, S. Shi, X. Zhu, L. He, J. Liao, and P. Zhuang, Phys. Rev. D **103**, 056025 (2021).
[66] N. Yamamoto and D.-L. Yang, Astrophys. J. **895**, 56 (2020).
[67] D.-L. Yang, K. Hattori, and Y. Hidaka, J. High Energy Phys. 07 (2020) 070.
[68] Z. Wang and P. Zhuang, arXiv:2105.00915.
[69] X.-L. Sheng, N. Weickgenannt, E. Speranza, D. H. Rischke, and Q. Wang, Phys. Rev. D **104**, 016029 (2021).
[70] X.-L. Luo and J.-H. Gao, J. High Energy Phys. 11 (2021) 115.
[71] N. Weickgenannt, E. Speranza, X.-l. Sheng, Q. Wang, and D. H. Rischke, Phys. Rev. D **104**, 016022 (2021).
[72] Y. Hidaka, S. Pu, Q. Wang, and D.-L. Yang, Prog. Part. Nucl. Phys. **127**, 103989 (2022).
[73] S. Fang, S. Pu, and D.-L. Yang, Phys. Rev. D **106**, 016002 (2022).
[74] J.-H. Gao, Z.-T. Liang, and Q. Wang, Int. J. Mod. Phys. A **36**, 2130001 (2021).
[75] B. I. Abelev *et al.* (STAR Collaboration), Phys. Rev. Lett. **103**, 251601 (2009).
[76] B. I. Abelev *et al.* (STAR Collaboration), Phys. Rev. C **81**, 054908 (2010).
[77] G. Wang (STAR Collaboration), Nucl. Phys. **A904–905**, 248c (2013).
[78] L. Adamczyk *et al.* (STAR Collaboration), Phys. Rev. C **88**, 064911 (2013).
[79] L. Adamczyk *et al.* (STAR Collaboration), Phys. Rev. C **89**, 044908 (2014).
[80] L. Adamczyk *et al.* (STAR Collaboration), Phys. Rev. Lett. **113**, 052302 (2014).
[81] P. Tribedy (STAR Collaboration), Nucl. Phys. **A967**, 740 (2017).
[82] J. Adam *et al.* (STAR Collaboration), Phys. Lett. B **798**, 134975 (2019).
[83] B. Abelev *et al.* (ALICE Collaboration), Phys. Rev. Lett. **110**, 012301 (2013).
[84] V. Khachatryan *et al.* (CMS Collaboration), Phys. Rev. Lett. **118**, 122301 (2017).
[85] A. M. Sirunyan *et al.* (CMS Collaboration), Phys. Rev. C **97**, 044912 (2018).
[86] S. Pratt, S. Schlichting, and S. Gavin, Phys. Rev. C **84**, 024909 (2011).
[87] A. Bzdak, V. Koch, and J. Liao, Lect. Notes Phys. **871**, 503 (2013).
[88] N. N. Ajitanand, R. A. Lacey, A. Taranenko, and J. M. Alexander, Phys. Rev. C **83**, 011901 (2011).
[89] N. Magdy, S. Shi, J. Liao, N. Ajitanand, and R. A. Lacey, Phys. Rev. C **97**, 061901 (2018).
[90] A. H. Tang, Chin. Phys. C **44**, 054101 (2020).
[91] S. Schlichting and S. Pratt, Phys. Rev. C **83**, 014913 (2011).
[92] H.-J. Xu, X. Wang, H. Li, J. Zhao, Z-W. Lin, C. Shen, and F. Wang, Phys. Rev. Lett. **121**, 022301 (2018).
[93] H.-J. Xu, J. Zhao, Y. Feng, and F. Wang, Nucl. Phys. **A1005**, 121770 (2021).
[94] S. A. Voloshin, Phys. Rev. Lett. **105**, 172301 (2010).
[95] M. Abdallah *et al.* (STAR Collaboration), Phys. Rev. C **105**, 014901 (2022).
[96] Z.-T. Liang and X.-N. Wang, Phys. Rev. Lett. **94**, 102301 (2005); **96**, 039901(E) (2006).
[97] Z.-T. Liang and X.-N. Wang, Phys. Lett. B **629**, 20 (2005).
[98] J.-H. Gao, S.-W. Chen, W.-Tian Deng, Z.-T. Liang, Q. Wang, and X.-N. Wang, Phys. Rev. C **77**, 044902 (2008).
[99] L. Adamczyk *et al.* (STAR Collaboration), Nature (London) **548**, 62 (2017).
[100] I. Karpenko and F. Becattini, Eur. Phys. J. C **77**, 213 (2017).
[101] H. Li, L.-G. Pang, Q. Wang, and X.-L. Xia, Phys. Rev. C **96**, 054908 (2017).
[102] Y. Xie, D. Wang, and L. P. Csernai, Phys. Rev. C **95**, 031901 (2017).
[103] Y. Sun and C. M. Ko, Phys. Rev. C **96**, 024906 (2017).
[104] S. Shi, K. Li, and J. Liao, Phys. Lett. B **788**, 409 (2019).
[105] D.-X. Wei, W.-T. Deng, and X.-G. Huang, Phys. Rev. C **99**, 014905 (2019).
[106] H.-Z. Wu, L.-G. Pang, X.-G. Huang, and Q. Wang, Phys. Rev. Res. **1**, 033058 (2019).
[107] H.-Z. Wu, L.-G. Pang, X.-G. Huang, and Q. Wang, Nucl. Phys. **A1005**, 121831 (2021).
[108] B. Fu, K. Xu, X.-G. Huang, and H. Song, Phys. Rev. C **103**, 024903 (2021).
[109] S. Ryu, V. Jupic, and C. Shen, Phys. Rev. C **104**, 054908 (2021).

[110] X.-Y. Wu, C. Yi, G.-Y. Qin, and S. Pu, Phys. Rev. C **105**, 064909 (2022).
[111] Q. Wang, Nucl. Phys. **A967**, 225 (2017).
[112] F. Becattini and M. A. Lisa, Annu. Rev. Nucl. Part. Sci. **70**, 395 (2020).
[113] F. Becattini, Lect. Notes Phys. **987**, 15 (2021).
[114] J. Adam *et al.* (STAR Collaboration), Phys. Rev. Lett. **123**, 132301 (2019).
[115] S. Y. F. Liu and Y. Yin, Phys. Rev. D **104**, 054043 (2021).
[116] S. Y. F. Liu and Y. Yin, J. High Energy Phys. 07 (2021) 188.
[117] F. Becattini, M. Buzzegoli, and A. Palermo, Phys. Lett. B **820**, 136519 (2021).
[118] C. Yi, S. Pu, and D.-L. Yang, Phys. Rev. C **104**, 064901 (2021).
[119] C. Yi, S. Pu, J.-H. Gao, and D.-L. Yang, Phys. Rev. C **105**, 044911 (2022).
[120] B. Müller and A. Schäfer, Phys. Rev. D **98**, 071902 (2018).
[121] Y. Guo, S. Shi, S. Feng, and J. Liao, Phys. Lett. B **798**, 134929 (2019).
[122] M. Buzzegoli, arXiv:2211.04549.
[123] K. Xu, F. Lin, A. Huang, and M. Huang, Phys. Rev. D **106**, L071502 (2022).
[124] B. Fu, L. Pang, H. Song, and Y. Yin, arXiv:2201.12970.
[125] M. Aaboud *et al.* (ATLAS Collaboration), Nat. Phys. **13**, 852 (2017).
[126] J. Adam *et al.* (STAR Collaboration), Phys. Rev. Lett. **127**, 052302 (2021).
[127] W. Zha, J. D. Brandenburg, Z. Tang, and Z. Xu, Phys. Lett. B **800**, 135089 (2020).
[128] K. Hattori and K. Itakura, Ann. Phys. (Amsterdam) **330**, 23 (2013).
[129] K. Hattori and K. Itakura, Ann. Phys. (Amsterdam) **334**, 58 (2013).
[130] K. Hattori, H. Taya, and S. Yoshida, J. High Energy Phys. 01 (2021) 093.
[131] K. Hattori and K. Itakura, Ann. Phys. (Amsterdam) **446**, 169114 (2022).
[132] S. L. Adler, Ann. Phys. (N.Y.) **67**, 599 (1971).
[133] M. Aaboud *et al.* (ATLAS Collaboration), Phys. Rev. Lett. **121**, 212301 (2018).
[134] J. Adam *et al.* (STAR Collaboration), Phys. Rev. Lett. **121**, 132301 (2018).
[135] ALICE Collaboration, arXiv:2204.11732.
[136] M. Vidovic, M. Greiner, C. Best, and G. Soff, Phys. Rev. C **47**, 2308 (1993).
[137] K. Hencken, D. Trautmann, and G. Baur, Phys. Rev. A **51**, 1874 (1995).
[138] K. Hencken, G. Baur, and D. Trautmann, Phys. Rev. C **69**, 054902 (2004).
[139] W. Zha, L. Ruan, Z. Tang, Z. Xu, and S. Yang, Phys. Lett. B **781**, 182 (2018).
[140] J. D. Brandenburg *et al.*, arXiv:2006.07365.
[141] J. D. Brandenburg, W. Zha, and Z. Xu, Eur. Phys. J. A **57**, 299 (2021).
[142] C. Li, J. Zhou, and Y.-J. Zhou, Phys. Rev. D **101**, 034015 (2020).
[143] S. Klein, A. H. Mueller, B.-W. Xiao, and F. Yuan, Phys. Rev. Lett. **122**, 132301 (2019).
[144] S. Klein, A. H. Mueller, B.-W. Xiao, and F. Yuan, Phys. Rev. D **102**, 094013 (2020).
[145] C. Li, J. Zhou, and Y.-J. Zhou, Phys. Lett. B **795**, 576 (2019).
[146] B.-W. Xiao, F. Yuan, and J. Zhou, Phys. Rev. Lett. **125**, 232301 (2020).
[147] R.-j. Wang, S. Pu, and Q. Wang, Phys. Rev. D **104**, 056011 (2021).
[148] R.-j. Wang, S. Lin, S. Pu, Y.-f. Zhang, and Q. Wang, Phys. Rev. D **106**, 034025 (2022).
[149] S. Lin, R.-J. Wang, J.-F. Wang, H.-J. Xu, S. Pu, and Q. Wang, Phys. Rev. D **107**, 054004 (2023).
[150] P. F. Kolb, J. Sollfrank, and U. W. Heinz, Phys. Rev. C **62**, 054909 (2000).
[151] P. F. Kolb and U. W. Heinz, arXiv:nucl-th/0305084.
[152] Y. Hama, T. Kodama, and O. Socolowski, Jr., Braz. J. Phys. **35**, 24 (2005).
[153] P. Huovinen and P. V. Ruuskanen, Annu. Rev. Nucl. Part. Sci. **56**, 163 (2006).
[154] J.-Y. Ollitrault, Eur. J. Phys. **29**, 275 (2008).
[155] D. Teaney, Phys. Rev. C **68**, 034913 (2003).
[156] R. A. Lacey, N. N. Ajitanand, J. M. Alexander, P. Chung, W. G. Holzmann, M. Issah, A. Taranenko, P. Danielewicz, and H. Stöcker, Phys. Rev. Lett. **98**, 092301 (2007).
[157] C. Gale, S. Jeon, and B. Schenke, Int. J. Mod. Phys. A **28**, 1340011 (2013).
[158] S. Pu, V. Roy, L. Rezzolla, and D. H. Rischke, Phys. Rev. D **93**, 074022 (2016).
[159] V. Roy, S. Pu, L. Rezzolla, and D. Rischke, Phys. Lett. B **750**, 45 (2015).
[160] S. Pu and D.-L. Yang, Phys. Rev. D **93**, 054042 (2016).
[161] S. Pu and D.-L. Yang, EPJ Web Conf. **137**, 13021 (2017).
[162] I. Siddique, R.-j. Wang, S. Pu, and Q. Wang, Phys. Rev. D **99**, 114029 (2019).
[163] R.-j. Wang, P. Copinger, and S. Pu, Nucl. Phys. **A1005**, 121869 (2021).
[164] M. Shokri and N. Sadooghi, J. High Energy Phys. 11 (2018) 181.
[165] M. Shokri and N. Sadooghi, Phys. Rev. D **96**, 116008 (2017).
[166] G. Inghirami, L. D. Zanna, A. Beraudo, M. H. Moghaddam, F. Becattini, and M. Bleicher, Eur. Phys. J. C **76**, 659 (2016).
[167] R. Biswas, A. Dash, N. Haque, S. Pu, and V. Roy, J. High Energy Phys. 10 (2020) 171.
[168] Y. Jiang, S. Shi, Y. Yin, and J. Liao, Chin. Phys. C **42**, 011001 (2018).
[169] S. Shi, Y. Jiang, E. Lilleskov, and J. Liao, Ann. Phys. (Amsterdam) **394**, 50 (2018).
[170] S. Shi, Y. Jiang, E. Lilleskov, and J. Liao, Proc. Sci. CPOD2017 (**2018**) 021.
[171] D. Montenegro, L. Tinti, and G. Torrieri, Phys. Rev. D **96**, 076016 (2017).
[172] D. Montenegro, L. Tinti, and G. Torrieri, Phys. Rev. D **96**, 056012 (2017); **96**, 079901(A) (2017).
[173] W. Florkowski, B. Friman, A. Jaiswal, R. Ryblewski, and E. Speranza, Phys. Rev. D **97**, 116017 (2018).
[174] W. Florkowski, B. Friman, A. Jaiswal, and E. Speranza, Phys. Rev. C **97**, 041901 (2018).

[175] W. Florkowski, E. Speranza, and F. Becattini, Acta Phys. Pol. B **49**, 1409 (2018).
[176] W. Florkowski, A. Kumar, and R. Ryblewski, Prog. Part. Nucl. Phys. **108**, 103709 (2019).
[177] F. Becattini, W. Florkowski, and E. Speranza, Phys. Lett. B **789**, 419 (2019).
[178] D.-L. Yang, Phys. Rev. D **98**, 076019 (2018).
[179] W. Florkowski, A. Kumar, and R. Ryblewski, Phys. Rev. C **98**, 044906 (2018).
[180] W. Florkowski, A. Kumar, R. Ryblewski, and R. Singh, Phys. Rev. C **99**, 044910 (2019).
[181] K. Hattori, M. Hongo, X.-G. Huang, M. Matsuo, and H. Taya, Phys. Lett. B **795**, 100 (2019).
[182] W. Florkowski, A. Kumar, R. Ryblewski, and A. Mazeliauskas, Phys. Rev. C **100**, 054907 (2019).
[183] S. Bhadury, W. Florkowski, A. Jaiswal, A. Kumar, and R. Ryblewski, Phys. Lett. B **814**, 136096 (2021).
[184] S. Shi, C. Gale, and S. Jeon, Nucl. Phys. **A1005**, 121949 (2021).
[185] K. Fukushima and S. Pu, Lect. Notes Phys. **987**, 381 (2021).
[186] K. Fukushima and S. Pu, Phys. Lett. B **817**, 136346 (2021).
[187] S. Li, M. A. Stephanov, and H.-U. Yee, Phys. Rev. Lett. **127**, 082302 (2021).
[188] R. Singh, G. Sophys, and R. Ryblewski, Phys. Rev. D **103**, 074024 (2021).
[189] D. She, A. Huang, D. Hou, and J. Liao, Sci. Bull. **67**, 2265 (2022).
[190] A. D. Gallegos, U. Gürsoy, and A. Yarom, SciPost Phys. **11**, 041 (2021).
[191] M. Hongo, X.-G. Huang, M. Kaminski, M. Stephanov, and H.-U. Yee, J. High Energy Phys. 11 (2021) 150.
[192] W. Florkowski, R. Ryblewski, R. Singh, and G. Sophys, Phys. Rev. D **105**, 054007 (2022).
[193] D.-L. Wang, S. Fang, and S. Pu, Phys. Rev. D **104**, 114043 (2021).
[194] D.-L. Wang, X.-Q. Xie, S. Fang, and S. Pu, Phys. Rev. D **105**, 114050 (2022).
[195] S. Bhadury, W. Florkowski, A. Jaiswal, A. Kumar, and R. Ryblewski, Phys. Rev. Lett. **129**, 192301 (2022).
[196] R. Biswas, A. Daher, A. Das, W. Florkowski, and R. Ryblewski, arXiv:2211.02934.
[197] Z. Cao, K. Hattori, M. Hongo, X.-G. Huang, and H. Taya, Prog. Theor. Exp. Phys. **2022**, 071D01 (2022).
[198] Y.-C. Liu and X.-G. Huang, Nucl. Sci. Tech. **31**, 56 (2020).
[199] L. Yan and X.-G. Huang, arXiv:2104.00831.
[200] J.-J. Zhang, H.-Z. Wu, S. Pu, G.-Y. Qin, and Q. Wang, Phys. Rev. D **102**, 074011 (2020).
[201] J.-J. Zhang, X.-Li Sheng, S. Pu, J.-N. Chen, G.-L. Peng, J.-G. Wang, and Q. Wang, Phys. Rev. Res. **4**, 033138 (2022).
[202] Z. Wang, J. Zhao, C. Greiner, Z. Xu, and P. Zhuang, Phys. Rev. C **105**, L041901 (2022).
[203] G. Aarts, C. Allton, J. Foley, S. Hands, and S. Kim, Phys. Rev. Lett. **99**, 022002 (2007).
[204] H. T. Ding, A. Francis, O. Kaczmarek, F. Karsch, E. Laermann, and W. Soeldner, Phys. Rev. D **83**, 034504 (2011).
[205] K. Tuchin, Adv. High Energy Phys. **2013**, 490495 (2013).
[206] M. Gedalin and I. Oiberman, Phys. Rev. E **51**, 4901 (1995).
[207] M. M. Caldarelli, O. J. Dias, and D. Klemm, J. High Energy Phys. 0904 (2009) 025.
[208] X.-G. Huang, M. Huang, D. H. Rischke, and A. Sedrakian, Phys. Rev. D **81**, 045015 (2010).
[209] D. T. Son and P. Surowka, Phys. Rev. Lett. **103**, 191601 (2009).
[210] D. T. Son and B. Z. Spivak, Phys. Rev. B **88**, 104412 (2013).
[211] S. Pu, J.-h. Gao, and Q. Wang, Phys. Rev. D **83**, 094017 (2011).
[212] S. Pu and J.-h. Gao, Central Eur. J. Phys. **10**, 1258 (2012).
[213] S. Pu, Relativistic fluid dynamics in heavy ion collisions, Ph.D thesis, Hefei, CUST, 2011, 1108.5828.
[214] J.-W. Chen, Y.-F. Liu, S. Pu, Y.-K. Song, and Q. Wang, Phys. Rev. D **88**, 085039 (2013).
[215] J. D. Bjorken, Phys. Rev. D **27**, 140 (1983).
[216] T. Csörgő, F. Grassi, Y. Hama, and T. Kodama, Phys. Lett. B **565**, 107 (2003).
[217] F. Becattini, V. Chandra, L. Del Zanna, and E. Grossi, Ann. Phys. (Amsterdam) **338**, 32 (2013).
[218] R.-h. Fang, J.-Y. Pang, Q. Wang, and X.-N. Wang, Phys. Rev. D **95**, 014032 (2017).
[219] V. E. Ambrus and M. N. Chernodub, Eur. Phys. J. C **82**, 61 (2022).
[220] M. N. Chernodub and V. E. Ambrus, Phys. Rev. D **103**, 094015 (2021).
[221] V. E. Ambrus, J. High Energy Phys. 08 (2020) 016.
[222] I. Siddique, X.-L. Sheng, and Q. Wang, Phys. Rev. C **104**, 034907 (2021).
[223] M. Abdallah *et al.* (STAR Collaboration), Phys. Rev. C **104**, 024902 (2021).
[224] J. Adam *et al.* (STAR Collaboration), Phys. Rev. C **98**, 014910 (2018).